Inorg. Chem. **2002**, *41*, 479–491

Dicopper(II) Complexes of H-BPMP-Type Ligands: pH-Induced Changes of Redox, Spectroscopic (^{19}F NMR Studies of Fluorinated Complexes), Structural Properties, and Catecholase Activities

C. Belle,* C. Beguin, I. Gautier-Luneau, S. Hamman, C. Philouze, J. L. Pierre, F. Thomas, and S. Torelli

Laboratoire de Chimie Biomimétique (LEDSS, UMR CNRS 5616), Université J. Fourier, BP 53, 38041 Grenoble Cedex 9, France

E. Saint-Aman

Laboratoire d'Electrochimie Organique et de Photochimie Redox (UMR CNRS 5630), Université J. Fourier, BP 53, 38041 Grenoble Cedex 9, France

M. Bonin

Institute of Crystallography, University of Lausanne, BSP, 1015 Lausanne, Switzerland

Received May 21, 2001

Substitution of the methyl group from the H-BPMP (HL_{CH_3}) ligand (2,6-bis[(bis(2-pyridylmethyl)amino)methyl]-4-methylphenol) by electron withdrawing (F or CF_3) or electron donating (OCH_3) groups afforded a series of dinucleating ligand (HL_{OCH_3}, HL_F, HL_{CF_3}), allowing one to understand the changes in the properties of the corresponding dicopper complexes. Dinuclear Cu^{II} complexes have been synthesized and characterized by spectroscopic (UV–vis, EPR, ^{1}H NMR) as well as electrochemical techniques and, in some cases, by single-crystal X-ray diffraction: $[Cu_2(L_{OCH_3})(\mu OH)][(ClO_4)_2]\cdot C_4H_8O$, $[Cu_2(L_F)(\mu OH)][(ClO_4)_2]$, $[Cu_2(L_F)(H_2O)_2][(ClO_4)_3]\cdot C_3D_6O$, and $[Cu_2(L_{CF_3})(H_2O)_2][(ClO_4)_3]\cdot 4H_2O$. Significant differences are observed for the Cu–Cu distance in the two μ-hydroxo complexes (2.980 Å (R = OCH_3) and 2.967 Å (R = F)) compared to the two bis aqua complexes (4.084 Å (R = F) and 4.222 Å (R = CF_3)). The μ-hydroxo and bis aqua complexes are reversibly interconverted upon acid/base titration. In basic medium, new species are reversibly formed and identified as the bis hydroxo complexes except for the complex from HL_{CF_3} which is irreversibly transformed near pH = 10. pH-driven interconversions have been studied by UV–vis, EPR, and ^{1}H NMR, and the corresponding p*K* are determinated. In addition, with the fluorinated complexes, the changes in the coordination sphere around the copper centers and in their redox states are evidenced by the fluorine chemical shift changes (^{19}F NMR). For all the complexes described here, investigations of the catechol oxidase activities (oxidation of 3,5-di-*tert*-butylcatechol to the corresponding quinone) are of interest in modeling the catecholase enzyme active site and in understanding aspects of structure/reactivity. These studies show the pH-dependence for the catalytic abilities of the complexes, related with changes in the coordination sphere of the metal centers: only the μ-hydroxo complexes from HL_{CH_3}, HL_F, and HL_{OCH_3} exhibit a catecholase activity. Modification on R-substituent induces a drastic effect on the catecholase activity: the presence of an electron donating group on the ligand increases this activity; the reverse effect is observed with an electron withdrawing group.

Introduction

Many metalloenzymes contain in their active site two copper ions that operate cooperatively.[1] Consequently dinuclear copper complexes with two metal ions in close proximity have received a great deal of attention.[1−5] These complexes are particularly of interest in relation to their potential uses as bimetallic catalysts, mimicking the activity of enzymes.[6] In enzymes, the structural aspects of the active

* Author to whom correspondence should be addressed. E-mail: Catherine.Belle@ujf-grenoble.fr.

10.1021/ic010534g CCC: $22.00
Published on Web 01/11/2002

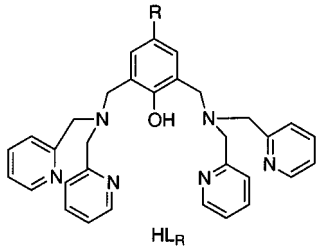

Figure 1. Dinucleating ligands HL_R employed to prepare the copper(II) complexes: R = CH_3 (HL_{CH_3}), F (HL_F), CF_3 (HL_{CF_3}), and OCH_3 (HL_{OCH_3}).

site dictate the type of activity.[7] Modeling the enzymes features requires the control of the interaction of the two metal centers. As a consequence, the design of the binucleating ligand has to satisfy a number of conditions: metal−metal distance, steric, electronic, and bridging ligand features, etc. In a previous paper,[8] we have described the pH-controlled changes of the metal coordination in a dicopper(II) complex of the ligand H-BPMP (2,6-bis[(bis(2-pyridylmethyl)amino)methyl]-4-methylphenol, HL_{CH_3}. We have shown that the catecholase activity of this complex was drastically dependent on the copper−copper distance, which was modified upon pH-induced changes in the coordination sphere of the complex. Spectroscopic features (UV−vis, EPR, and magnetic properties) and redox potentials are directly related to the structural aspects. For a better understanding of the various parameters that dictate the structural properties and the reactivity, we have prepared and studied dicopper complexes of new ligands derived from H-BPMP, bearing respectively strong electron withdrawing or donating groups in the 4-position of the phenol moiety (Figure 1).

Experimental Section

Commercial reagents (from Aldrich) were used as obtained without further purification. Solvents were purified by standard methods before use. Elemental analyses were performed by the CNRS Microanalysis Laboratory of Lyon, France.

Caution: Although no problems were encountered, suitable care and precautions should be taken when handling the perchlorate salts.

Spectrometry. Mass spectra were recorded on a Nermag R 1010C apparatus. Fast-atom bombardment (FAB) in the positive mode were obtained with the spectrometer equipped with a M scan (Wallis) atom gun (8 kV, 20 mA). UV−visible spectra were obtained using a UVIKON 930 spectrophotometer operating in the range 200−900 nm with quartz cells. ϵ are given in $M^{-1}\cdot cm^{-1}$. The deprotonation constants were determined in aqueous solutions (2.5×10^{-4} M); the ionic strength was adjusted with 0.01 M $NaClO_4$ in acidic medium. EPR spectra were recorded at 100 K on a BRUKER ESP 300E spectrometer operating at 9.4 GHz (X-band), with 3 mM solutions in H_2O−DMSO (dimethyl sulfoxide; 1/1 (v/v)). ^1H NMR spectra were recorded on a BRUKER AC 200, WM 250, or Avance 300 spectrometer at 25 °C. Chemical shifts (ppm) were referenced to residual solvent peaks. ^{19}F NMR were recorded on a Bruker Avance 300 (282.39 MHz) or AC 200 (188.36 MHz) spectrometer. ^{19}F chemical shifts are expressed with respect to C_6F_6.

Electrochemistry. Electrochemical experiments were carried out using a PAR model 273 potentiostat equipped with a Kipp-Zonen *x*−*y* recorder. All experiments were run at room temperature under argon atmosphere. For analytical experiments, a standard three-electrode cell was used. Potentials are referred to an Ag/10 mM $AgNO_3$ reference electrode with 0.1 M tetra-*n*- butylammonium perchlorate (TBAP) as supporting electrolyte. Vitrous carbon disk electrodes for cyclic voltammetry (CV; 5 mm diameter) and rotating disk electrode (RDE; 3 mm diameter) were polished with 1 μm diamond paste

X-ray Data Collections and Crystal Structure Determinations. Crystal data, together with details of diffraction experiment and refinement, are summarized in Table 1.

The crystal of complex $[Cu_2(L_{OCH_3})(\mu\text{-}OH)]^{2+}$ merits some comments. Indeed, optical observations under polarizing microscope revealed the systematic twinned character of this compound. After a careful selection, one specimen constituted by two large orientational domains was isolated and gently cut in order to obtain a sample of sufficient size as a monodomain as possible. The crystal was mounted on Stoe IPDS diffractometer, using Mo Kα graphite-monochromated radiation (λ = 0.710 73 Å). A preliminary data collection revealed the persisting presence of a minor twin component which is leading to a twin-lattice quasi-symmetry.[9a,b] Optimization of data collection parameters, especially the crystal-detector distance and the temperature (120 K), was performed. The three-dimensional reciprocal view resulting from the full intensity data collection confirmed the mainly monodomain character of the sample. Using the Stoe IPDS software package[9c] gave a pretty good data set from the major twin component corresponding to about 85% of the total diffracting volume. The twin mirror plane is perpendicular to *c* and generates a twin obliquity[9a,b] about 2.5° in the *ac* plane.

The crystals of complexes $[Cu_2(L_F)(\mu\text{-}OH)]^{2+}$, $[Cu_2(L_F)(H_2O)_2]^{3+}$, and $[Cu_2(L_{CF_3})(H_2O)_2]^{3+}$ were mounted on a Enraf-Nonius CAD4 diffractometer using a graphite crystal monochromator (λ(Mo Kα) = 0.710 73 Å), at 293 K. The reflections were corrected for Lorentz and polarization effects but not for absorption. Each structure was solved by direct methods and refined using TEXSAN software.[9d]

All non-hydrogen atoms were refined with anisotropic thermal parameters. Hydrogen atoms were generated in idealized positions, riding on the carrier atoms, with isotropic thermal parameters, except for the hydrogen atoms of hydroxyl groups and of aqua ligands which were localized on difference Fourier map but not refined.

The crystal structures of the complexes $[Cu_2(L_{OCH_3})(\mu\text{-}OH)]^{2+}$, $[Cu_2(L_F)(\mu\text{-}OH)]^{2+}$, $[Cu_2(L_F)(H_2O)_2]^{3+}$, and $[Cu_2(L_{CF_3})(H_2O)_2]^{3+}$ give respectively the following formulas: $[Cu_2(OH)(C_{33}H_{33}N_6O_2)]$-

(1) Karlin, K. D.; Tyeklar, Z. *Bioinorganic Chemistry of Copper*; Chapman & Hill: New York, 1993.
(2) Karlin, K. D.; Zuberbühler, A. D. In *Bioinorganic Catalysis*; Reedjik, J., Bouwman, E., Eds.; Marcel Dekker: New York, 1999; pp 469−534.
(3) Sorrell, T. N. *Tetrahedron* **1989**, *45*, 3−68.
(4) Vigato, P. A.; Tamburini, S.; Fenton, D. *Coord. Chem. Rev.* **1990**, *106*, 25−170.
(5) Kitajima, N. *Adv. Inorg. Chem.* **1992**, *39*, 1−77.
(6) Van den Beuken, E. K.; Feringa, B. L. *Tetrahedron* **1998**, *54*, 12985−13011.
(7) Solomon, E. I.; Sundaram, U. M.; Machonkin, T. E. *Chem. Rev.* **1996**, *96*, 2563−2605.
(8) Torelli, S.; Belle, C.; Gautier-Luneau, I.; Pierre, J. L.; Saint-Aman, E.; Latour, J. M.; Le Pape, L.; Luneau, D. *Inorg. Chem.* **2000**, *39*, 16, 3526−3536.
(9) (a) Donnay, G.; Donnay, J. D. H. *Can. Mineral.* **1974**, *12*, 422−425. (b) Le Page, Y.; Donnay, J. D. H.; Donnay, G. *Acta Crystallogr.* **1984,** *A40*, 679−684. (c) CELL, INTEGRATE and RECIPE. *Stoe IPDS software package*, Version 2.87; Stoe & CIE GmbH: Darmstadt, Germany, 1997. (d) TEXSAN. *Single-Crystal Structure Analysis Software*, Version 1.7; MSC, Molecular Structure Corp.: The Woodlands, TX, 1995.

Table 1. Crystal Data and Structure Refinement Details

	$[Cu_2(L_{OCH_3})(\mu\text{-}OH)]^{2+}$	$[Cu_2(L_F)(\mu\text{-}OH)]^{2+}$	$[Cu_2(L_F)(H_2O)_2]^{3+}$	$[Cu_2(L_{CF_3})(H_2O)_2]^{3+}$
empirical formula	$Cu_2C_{33}H_{34}N_6O_3{\cdot}(ClO_4)_2{\cdot}C_4H_8O$	$Cu_2C_{32}H_{31}N_6O_2F{\cdot}(ClO_4)_2$	$Cu_2C_{32}H_{34}N_6O_3F{\cdot}(ClO_4)_3{\cdot}C_3D_6O$	$Cu_2C_{33}H_{34}N_6O_3F_3{\cdot}(ClO_4)_3{\cdot}4H_2O$
fw ($g{\cdot}mol^{-1}$)	960.77	876.63	1059.18	1117.16
cryst syst	monoclinic	monoclinic	orthorhombic	orthorhombic
space group	$P2_1/c$	$P2_1/c$	$Pna2_1$	Pbcn
a (Å)	13.278(3)	11.641(4)	12.569(6)	16.125(5)
b (Å)	16.786(3)	22.080(10)	18.423(9)	16.553(5)
c (Å)	17.673(4)	14.161(3)	18.919(9)	16.822(4)
β (deg)	91.25(3)	105.00(2)		
V ($Å^3$)/Z	3938(1)/4	3516(2)/4	4381(3)/4	4490(2)/4
D_x ($g{\cdot}cm^{-3}$)	1.620	1.656	1.609	1.653
μ (cm^{-1})	12.87	14.33	12.33	12.19
cryst dimen (mm)	0.06 × 0.14 × 0.24	0.2 × 0.15 × 0.3	0.15 × 0.15 × 0.3	0.1 × 0.3 × 0.3
shape/color	platelet/emerald green	platelet/olive green	needle/deep blue	platelet/green-blue
diffractometer	STOE- IPDS	CAD4-Enraf Nonius	CAD4-Enraf Nonius	CAD4-Enraf Nonius
T (K)	120	293	293	293
$2\theta_{max}$ (deg)	56	50	60	60
no. of reflcns collctd	26 644	12 699	7009	7178
no. of unique reflcns	7869	9786	7009	7178
no. of reflcns used	5296 [$F > 2\sigma(F)$]	2984 [$F > \sigma(F)$]	3660 [$F > \sigma(F)$]	2921 [$F > 2\sigma(F)$]
no. of params refined	532	478	568	318
$R(F)^a$	0.0579	0.0595	0.064	0.0698
$R_w(F)^b$	0.0626	0.0657	0.039	0.0721
fudge factor p	2.4×10^{-4}	3.0×10^{-4}	1.4×10^{-4}	4.0×10^{-4}
goodness of fit S	1.95	1.89	1.97	1.99
$\Delta\rho_{min}/\Delta\rho_{max}$ ($e{\cdot}Å^{-3}$)	−0.86/0.91	−0.65/1.34	−0.74/0.66	−0.55/0.6

[a] $R = \sum||F_o| - |F_c||/\sum|F_o|$. [b] $R_w = [\sum(|F_o| - |F_c|)^2/\sum wF_o^2]^{1/2}]$ with $w = 1/[\sigma^2(F_o) + p|F_o|^2]$.

$(ClO_4)_2{\cdot}(C_4H_8O)$; $[Cu_2(OH)(C_{32}H_{30}N_6OF)](ClO_4)_2$; $[Cu_2(C_{32}H_{30}N_6OF)(H_2O)_2](ClO_4)_3{\cdot}C_3D_6O$; and $[Cu_2(C_{33}H_{30}N_6OF_3)(H_2O)_2](ClO_4)_3{\cdot}4H_2O$.

The crystal structure of the last complex reveals that the tricationic molecular entity is lying on a 2-fold axis with the atoms O1, C1, C4, and C5 sitting at special positions. So only half of a molecular unit, 1.5 perchlorate anions, and two water solvent molecules have been defined. One perchlorate anion is in general position.The other is close to the 2-fold axis, so that the chlorine atom and two oxygen atoms were refined with a site occupation factor (sof) of 0.5 and one oxygen atom with a sof of 1.

Syntheses. (a) Ligands. (1) HL_{OCH_3}[10] was synthesized according to the preparation previously described.

(2) 2,6-Bis(hydroxymethyl)-4-fluorophenol (1a). To 4-fluorophenol (11.2 g, 100 mmol) in 30 mL of methanol was added drop by drop 50 mL of an aqueous solution of NaOH (25% (w/w)). After 30 mn of stirring, 90 mL of formaldehyde (37% (w/w) in methanol) was added dropwise. The resulting mixture was refluxed during 3 days. Then, the solution was adjusted to pH 5 (0 °C) by addition of a mixture of glacial acetic acid (15 mL) in water (30 mL). Evaporation of the solvent yielded a solid. After addition of 150 mL of water, the product was extracted with ethyl acetate (3 × 200 mL). The combined organic layers were dried over Na_2SO_4, and the solvent was removed to yield the crude product. Recristallization in diethyl ether afforded **1a** as white solid (12.2 g, 71% yield). Mp: 130 °C (lit.[11] 137−139 °C). ^1H NMR (250 MHz, DMSO-d_6, TMS): δ 4.60 (s, 4H, $-CH_{2-}$); 5.51 (s,1H, −OH); 6.90 (d, J = 9.5 Hz, 2H, H_{arom}). ^{13}C NMR (62.5 MHz, DMSO, TMS): δ 156.1 (d, J^1(C−F) = 232 Hz); 146.9; 130.9 (d, J^3(C−F) = 6.5 Hz); 111.3 (d, J^2(C−F) = 23.8 Hz); 52.7. ^{19}F NMR (188.36 MHz, DMSO, C_6F_6): δ 38.08 (t, J = 9.5 Hz). Anal. Calcd for $C_8H_9O_3F$: C, 55.80; H, 5.27; F, 10.79. Found: C, 55.75; H, 5.30; F, 10.84. MS (DCI, NH_3, isobutane): m/z = 190 $[M + NH_4]^+$; 172 $[M]^+$. IR (KBr): 1180 cm^{-1} (Ar−F).

(3) 2,6-Bis(chloromethyl)-4-fluorophenol (1b). To a solution of **1a** (1 g, 4.8 mmol) in 10 mL of dry CH_2Cl_2, was added dropwise freshly distilled thionyl chloride (5.7 g, 48 mmol) in 15 mL of CH_2Cl_2 under a dinitrogen atmosphere. After 1 h, the volatiles were removed in vacuo to yield a crude solid. The product was washed with hexane and used without purification (1.2 g, 98% yield). An analytical sample of **1b** was obtained by flash column chromatography on silica gel (ethyl acetate/pentane, 1/2): Mp = 58 °C. ^1H NMR (250 MHz, $CDCl_3$, TMS): δ 7.03 (d, J = 8.2 Hz, 2H, H_{arom}) 5.54 (s,1H, −OH) 4.64 (s, 4H, $-CH_2$). ^{13}C NMR (62.5 MHz, $CDCl_3$, TMS): δ 156.4 (d, J^1(C−F) = 266 Hz); 148.9; 126.3 (d, J^3(C−F) = 9.4 Hz); 117.2 (d, J^2(C−F) = 29.4 Hz); 41.6. ^{19}F NMR (188.36 MHz, $CDCl_3$, C_6F_6): δ 39.90 (t, J = 8.2 Hz). Anal. Calcd for $C_8H_7OFCl_2$: C, 45.74; H, 3.41; F, 9.09; Cl, 33.52. Found: C, 45.79; H, 3.38; F, 8.97; Cl, 33.62. IR (KBr, cm^{-1}: 1187 (Ar−F)). MS (DCI, NH_3, isobutane): m/z = 227 $[M + NH_4]^+$; 209 $[M]^+$.

(4) 2,6-Bis(bis(2-pyridylmethyl)aminomethyl)-4-fluorophenol (HL_F). Under a dinitrogen atmosphere, a mixture of bis(2-pyridylmethyl)amine (5.8 g, 29 mmol) and triethylamine (5.6 g, 58 mmol) in 30 mL of dry tetrahydrofuran (THF) was added dropwise to a stirred solution of **1b** (3 g, 14.35 mmol) in 15 mL of dry THF at 0 °C. Then, the resulting mixture was allowed to warm to room temperature. After 3 days, the resulting suspension was filtered, and the filtrate was concentrated under reduced pressure. The residue was dissolved in 100 mL of methylene chloride, washed with brine, and dried over anhydrous Na_2SO_4. The solution was evaporated to dryness under reduced pressure, and a crude product was obtained as a brown oil (8.4 g). Chromatography on silica gel (acetone) afforded 5.5 g (71% yield) of HL_F as a yellow solid. ^1H NMR (300 MHz, $CDCl_3$, TMS): δ 3.78 (s, 4H, Ar−CH_{2-}N); 3.87 (s, 8H, Py−CH_{2-}); 6.98 (d, J = 11.0 Hz, 2H, CH−CF); 7.13 (m, 4H, CH_{arom}); 7.48 (m, 4H, CH_{arom}); 7.60 (m, 4H, CH_{arom}); 8.52 (d, J = 9 Hz, 4H, o-H−Py); 11.10 (s, 1H, −OH). ^{13}C NMR (62.5 MHz, $CDCl_3$, TMS): δ 157.3; 157.0 (d, J^1(C−F) = 248 Hz); 151.5; 148.7; 136.4; 125.3 (d, J^3(C−F) = 6.8 Hz); 123.6; 122.7; 114.7

(10) Albedyhl, S.; Averbuch-Pouchot, M. T.; Belle, C.; Krebs, B.; Pierre, J. L.; Saint-Aman, E.; Torelli, S. *Eur. J. Inorg. Chem.* **2001**, 1457−1464.

(11) Moshfegh, A. A.; Mazandarini, B.; Nahid, A.; Hakimelahi, G. H. *Helv. Chim. Acta* **1982**, *65*, 1229−1232.

(d, J^3(C−F) = 20.6 Hz); 59.6; 54.2. ^{19}F NMR (188.36 MHz, $CDCl_3$, C_6F_6): δ 32.00 (t, J = 10.9 Hz). Anal. Calcd for $C_{32}H_{31}N_6OF$: C, 71.89; H, 5.84; N, 15.72; F, 3.55. Found: C, 71.93; H, 5.87; N, 15.78; F, 3.49. MS (DCI, NH_3, isobutane): m/z = 535 $[M + H]^+$. IR (KBr, cm^{-1}): 1187 (Ar−F)).

(5) 2,6-Bis(bis(2-pyridylmethyl)aminomethyl)-4-trifluoromethylphenol (HL_{CF_3}). To 4-trifluoromethylphenol (1 g, 6.13 mmol) in 50 mL of absolute ethanol were added bis(2-pyridylmethyl)amine (2.84 g, 14 mmol) and *para*-formaldehyde (0.5 g, 16.6 mmol). The mixture was refluxed for 5 days and the solvent removed in vacuo. The resulting oil was taken up in CH_2Cl_2/10% $NaHCO_3$ solution, and the layers were separated. The aqueous solution was then extracted with CH_2Cl_2 (4 × 40 mL), and the combined organic layers were dried over Na_2SO_4. Evaporation of the solvent yielded a crude orange oil which was purified by chromatography on silica gel (acetone) to afford 2.72 g (75% yield) of HL_{CF_3} as a yellow oil. ^{1}H NMR (200 MHz, $CDCl_3$, TMS): δ 3.86 (s, 4H, Ar−CH_2–N); 3.90 (s, 8H, Py−CH_2–N); 7.02 (d, J = 11.0 Hz, 2H, CH_{arom}); 7.12 (m, 4H, CH_{arom}); 7.50 (m, 4H, CH_{arom}); 7.70 (m, 4H, CH_{arom}); 8.51 (d, J = 9.2 Hz, 4H, *o*-H−Py) and 11.00 (s, 1H, −OH). ^{13}C NMR (50 MHz, $CDCl_3$, TMS): δ 158.8; 157.0 (d, J^4(C−F) = 248 Hz); 151.5; 148.7; 136.4; 125.3 (d, J^3(C−F) = 6.8 Hz); 123.6; 122.7; 114.7 (d, J^2(C−F) = 20.6 Hz); 59.7 and 54.3.^{19}F NMR (188.36 MHz, $CDCl_3$, C_6F_6): δ 100.75 (s). IR (KBr, cm^{-1}): 1187 (Ar−F). MS (DCI, NH_3, isobutane): m/z = 585 $[M + H]^+$. Anal. Calcd. for $C_{33}H_{31}N_6OF_3$: C, 67.80; H, 5.34; N, 14.37; F, 9.75. Found: C, 67.77; H, 5.37; N, 14.39; F, 9.69.

(b) Complexes. (1) $[Cu_2(L_F)(\mu\text{-OH})](ClO_4)_2$. To 100 mg (0.187 mmol) of HL_F dissolved in CH_3CN (15 mL) with 53 μL (0.364 mmol) of Et_3N, a solution of 170 mg of $Cu(ClO_4)_2\cdot 6H_2O$ (0.374 mmol) in CH_3CN (5 mL) was added dropwise. The initial yellow solution turned green and was stirred for 1 h. Then the solvent was partially removed under reduced pressure. To the resulting solution (10 mL) was added some amount of THF, and the mixture was allowed to stand 4 days at −20 °C. A 122 mg amount of a green powder were collected by filtration (75% yield). Crystals of X-ray quality were obtained by vapor diffusion of THF in an acetonitrile solution. Anal. Calcd for $C_{32}H_{31}N_6O_{10}FCu_2Cl_2$: C, 43.84; H, 3.56; N, 9.59; F, 2.17; Cu, 14.50; Cl, 8.09. Found: C, 44.18; H, 3.68; N, 10.09; F, 1.93; Cu, 13.75; Cl, 7.69. UV−vis in CH_3CN: λ_{max} = 312 (ϵ = 4910), 410 nm (sh, ϵ = 440), 781 nm (ϵ = 260). FAB-MS (Matrix NBA): m/z = 859 $[L_F + 2Cu + 2ClO_4 + H]^+$; 659 $[L_F + 2Cu + H]^+$.

(2) $[Cu_2(L_{CF_3})(\mu\text{-OH})](ClO_4)_2$. This compound was prepared from HL_{CF_3} (100 mg, 0.171 mmol), Et_3N (50 μL, 0.342 mmol) and $Cu(ClO_4)_2\cdot 6H_2O$ (130 mg, 0.342 mmol) by an analogous procedure to that used to prepare $[(Cu_2(L_F)(\mu\text{-OH})](ClO_4)_2$. Green crystals suitable for of X-ray crystallography were obtained by vapor diffusion of THF in an acetonitrile solution. Anal. Calcd for $C_{33}H_{31}N_6O_{10}F_3Cu_2Cl_2$: C, 42.77; H, 3.47; N, 9.17; F, 6.15; Cu, 12.72; Cl, 7.65. Found: C, 42.45; H, 3.69; N, 9.35; F, 6.07; Cu, 12.58; Cl, 7.87. UV−vis in CH_3CN: λ_{max} = 300 (ϵ = 251), 340 nm (sh, ϵ = 760), 806 nm (ϵ = 251). FAB-MS (Matrix NBA): m/z = 810 $[L_{CF_3}+ 2Cu + ClO_4 + H]^+$.

(3) $[Cu_2(L_{OCH_3})(\mu\text{-OH})](ClO_4)_2$. This compound was prepared from HL_{OCH_3} (200 mg, 0.36 mmol), Et_3N (100 μL, 0.684 mmol) and $Cu(ClO_4)_2\cdot 6H_2O$ (291 mg, 0.766 mmol) by an analogous procedure to that used to prepare $[Cu_2(L_F)(\mu\text{-OH})](ClO_4)_2$. Green crystals suitable for X-ray were obtained by vapor diffusion of THF in a solution of CH_3CN. Anal. Calcd for $C_{33}H_{34}N_6O_{11}Cu_2Cl_2$: C, 44.60; H, 3.86; N, 9.46; Cu, 14.30; Cl, 7.98. Found: C, 44.04; H, 4.09; N, 9.28; Cu, 13.92; Cl, 8.64. UV−vis in CH_3CN: λ_{max} = 315 nm (ϵ = 5300), 440 nm (sh, ϵ = 560), 787 nm (ϵ = 300). FAB-MS (Matrix NBA) m/z = 663 $[L_{OCH_3} + 2Cu + H]^+$.

(4) $[Cu_2(L_F)(H_2O)_2](ClO_4)_3$. To 100 mg (0.187 mmol) of HL_F in distilled water (15 mL) and acetone (5 mL) were added dropwise 170 mg of $Cu(ClO_4)_2\cdot 6H_2O$ (0.374 mmol) in water (5 mL). The solution turned brown instantaneously and was stirred for 1 h at room temperature and then heated to remove acetone. The resulting solution was allowed to stand at 4 °C for 12 days. A green powder was recovered (150 mg, 80% yield). Blue-green crystals suitable for X-ray were obtained by slow evaporation of a solution of $[Cu_2(L_F)(H_2O)_2](ClO_4)_3$ in acetone-d_6. Anal. Calcd for $C_{32}H_{34}N_6O_{15}FCu_2Cl_3\cdot 3H_2O$: C, 36.63; H, 3.84; N, 8.01; F,1.81; Cu, 12.11; Cl, 10.14. Found: C, 36.72; H, 3.85; N, 7.77; F, 1.47; Cu, 11.46; Cl, 9.34. UV−vis in H_2O: λ_{max} = 301 nm (ϵ = 3215), 441 nm (ϵ = 555), 693 nm (ϵ = 253). FAB-MS (Matrix NBA): m/z = 859 $[L_F + 2Cu + 2ClO_4 + H]^+$; 659 $[L_F + 2Cu + H]^+$.

(5) $[Cu_2(L_{CF_3})(H_2O)_2](ClO_4)_3$. This compound was prepared from HL_{CF_3} (100 mg, 0.171 mmol) and $Cu(ClO_4)_2\cdot 6H_2O$ (130 mg, 0.342 mmol) by an analogous procedure to that used for $[Cu_2(L_F)(H_2O)_2](ClO_4)_3$. Green crystals suitable for X-ray were obtained by slow evaporation of an aqueous solution. Anal. Calcd for $C_{33}H_{34}N_6O_{15}F_3Cu_2Cl_3\cdot 6H_2O$: C, 34.37; H, 4.02; N, 7.29; F, 4.94; Cu, 11.02; Cl, 9.22. Found: C, 35.01; H, 3.94; N, 7.21; F, 4.75; Cu, 10.53; Cl, 9.13. UV−vis in H_2O: λ_{max} = 286 nm (ϵ = 4524), 380 nm (ϵ = 395), 701 nm (ϵ = 265). FAB-MS (Matrix NBA): m/z = 908 $[L_{CF_3} + 2Cu + 2ClO_4 + H]^+$.

(6) $[Cu_2(L_{OCH_3})(H_2O)_2](ClO_4)_3$. This compound was prepared from HL_{OCH_3} (100 mg, 0.187 mmol) and $Cu(ClO_4)_2\cdot 6H_2O$ (138 mg, 0.374 mmol) by the same procedure used for $[Cu_2(L_F)(H_2O)_2](ClO_4)_3$. Blue crystals suitable for X-ray were obtained by slow evaporation of an aqueous solution. Anal. Calcd for $C_{33}H_{37}N_6O_{16}Cu_2Cl_3\cdot 4H_2O$: C, 36.73; H, 4.20; N, 7.79; Cu, 11.78; Cl, 9.86. Found: C, 37.41; H, 4.47; N, 8.01; Cu, 10.98; Cl, 9.03. UV−vis in H_2O: λ_{max} = 460 nm (ϵ = 720), 691 nm (ϵ = 363). FAB-MS (Matrix NBA): m/z = 971 $[L_{OCH_3} + 2Cu + 2ClO_4 + H]^+$; 772 $[L_{OCH_3} + 2Cu + ClO_4 + H]^+$.

Catecholase Activities. The catecholase activity of the complexes described herein has been evaluated at 25 °C by reaction with 3,5-di-*tert*-butylcatechol (3,5-DTBC). The absorption at λ_{max} = 410 nm (ϵ = 1900), characteristic of the formed quinone, was measured as a function of time. A 2.5 × 10^{-4} M solution of the complex with 100 equiv of 3,5-DTBC has been used. The experiments were run under 1 atm of dioxygen. Under these conditions, catechol was not oxidized in the absence of copper complexes. For the μ-OH complexes same results were obtained in CH_3CN or in a mixture (CH_3CN/H_2O, 20/80) buffered at pH = 7. For the bis H_2O or bis OH series, measurements were performed in a mixture CH_3CN/H_2O, 20/80. Under these conditions, no changes were observed in the UV−vis spectra of the initial solutions. The kinetic parameters were determined for 4.5 × 10^{-5} M solutions of complexes and 0.225 mM to 4.50 mM solutions of substrate.

Results and Discussion

Syntheses of Ligands and Dicopper(II) Complexes. The dinucleating ligands (HL_F, HL_{CF_3}, and HL_{OCH_3}) are prepared by standard methods, via the bishydroxymethylation of 4R-subtituted phenols (commercial for HL_{CH_3} preparation[8,12−13]). For HL_{OCH_3}[10] detailed synthesis has been previously de-

(12) Suzuki, M.; Kanatomi, H.; Murase, I. *Chem. Lett.* **1981**, 1745−1748.
(13) Borovik, A. S.; Papaefthymiou, V.; Taylor, L. F.; Anderson, O. P.; Que, L. *J. Am. Chem. Soc.* **1989**, *111*, 6183−6195.

scribed. For HL_F, reaction of 4-fluorophenol with CH_2O/NaOH affords 2,6-bis(hydroxymethyl)-4-fluorophenol (**1a**).[11] Subsequent substitution of the benzylic hydroxyl group by a chlorine using $SOCl_2$ (**1b**) and finally substitution of the benzylic chloride by *N*,*N*-bis(2-pyridyl)methylamine[8] afforded HL_F. Since 4-trifluorophenol is not stable in basic medium, HL_{CF_3} was prepared by diaminomethylation of 4-trifluorophenol in an aromatic Mannich reaction.[14]The dibridged dinuclear copper(II) complexes were prepared by the addition of 2 equiv of $Cu(ClO_4)_2 \cdot 6H_2O$ to the solution of appropriate ligand in acetonitrile containing 2 equiv of triethylamine. The monobridged dinuclear copper(II) complexes were prepared in a similar manner, in a acetone/water mixture and without triethylamine.

Description of Crystal Structures. (a) Complexes $[Cu_2(L_{OCH_3})(\mu\text{-OH})]^{2+}$ and $[Cu_2(L_F)(\mu\text{-OH})]^{2+}$. The ORTEP views of the dicationic complexes are shown in Figure 2A ($[Cu_2(L_{OCH_3})(\mu\text{-OH})]^{2+}$) and in Figure 2B ($[Cu_2(L_F)(\mu\text{-OH})]^{2+}$). Selected bond lengths and angles are given in Table 2. The crystal structures reveal in both cases that the copper atoms are doubly bridged by the phenoxo and by a hydroxo group. The pentacoordination of copper atoms is achieved by the tertiary amine and two pyridine nitrogens which are cis to each other. In both complexes, the coordination polyhedra are distorted trigonal bipyramids with atoms O1, N3, N4 and O1, N5, N6 forming the trigonal planes where Cu1 and Cu2 are respectively located at 0.160 and 0.141 Å out of the plane for $[Cu_2(L_{OCH_3})(\mu\text{-OH})]^{2+}$ and at 0.142 and 0.151 Å for $[Cu_2(L_F)(\mu\text{-OH})]^{2+}$ toward the O2 atom. The distances Cu−N and Cu−O are respectively in the ranges of 2.010(4)−2.245(4) and 1.905(3)−2.039(3) Å for $[Cu_2(L_{OCH_3})(\mu\text{-OH})]^{2+}$ and 2.004(6)−2.057(5) and 1.895(5)−2.123(5) Å for $[Cu_2(L_F)(\mu\text{-OH})]^{2+}$.

However, as seen on ORTEP views (Figure 2A,B), the conformation of the ligand is different for the two complexes. While the two nitrogen atoms N1 and N2 of the tertiary amines are in the trans position with regard to the plane of the phenoxo ring and benzylic carbons C8 and C9 for $[Cu_2(L_{OCH_3})(\mu\text{-OH})]^{2+}$, they are in the cis position for $[Cu_2(L_F)(\mu\text{-OH})]^{2+}$.

The complex $[Cu_2(L_{OCH_3})(\mu\text{-OH})]^{2+}$ is structurally very similar to the complex $[Cu_2(L_{CH_3})(\mu\text{-OH})]^{2+}$ previously described.[8] The four atoms Cu1, Cu2, O1, and O2 are in the same plane with a maximal deviation to the least-squares plane of 0.004(1) Å. The phenolate ring is both tilted to the O1−O2 axis and twisted with respect to the O1−Cu1−O2−Cu2 plane. The tilting is seen by measuring the angle O2−O1−C1 (146.6(3)°) compared to 151.7(5)° for $[Cu_2(L_{CH_3})(\mu\text{-OH})]^{2+}$ and the twisting from the torsion angles Cu1−O1−C1−C2 (11.7(3)°) and Cu2−O1−C1−C6 (−42.8(1)°). The angles in Cu_2O_2 unit are almost the same as those observed in the complex $[Cu_2(L_{CH_3})(\mu\text{-OH})]^{2+}$; the differences are less than 1°, whereas the mean distance Cu−O in Cu_2O_2 unit is slightly longer. This leads to an intermetallic distance Cu1···Cu2 of 2.980(9) Å longer than that of 2.966(1) Å observed in $[Cu_2(L_{CH_3})(\mu\text{-OH})]^{2+}$.[8]

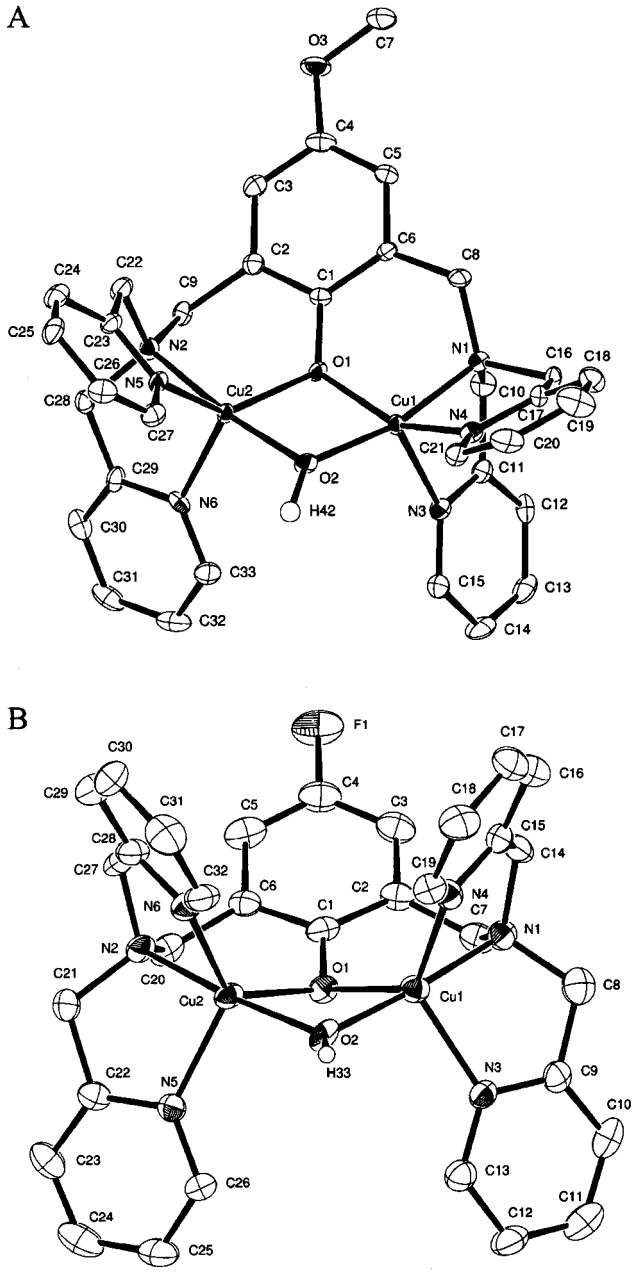

Figure 2. ORTEP plots of the dicationic units with atom labels and numbering scheme for (A) $[Cu_2(L_{OCH_3})(\mu OH)]^{2+}$ and (B) $[Cu_2(L_F)(\mu OH)]^{2+}$. Hydrogens are omitted for clarity, except for hydroxy groups. Ellipsoids are drawn at the 30% probability level.

In the complex $[Cu_2(L_F)(\mu\text{-OH})]^{2+}$ a pseudo-mirror appears going through the F1, C4, C1, O1, and O2 atoms, leading to a butterfly shape for the Cu_2O_2 unit. The dihedral angle between the planes Cu1−O1−O2 and Cu2−O1−O2 is 151.6°. Except the Cu1−O1−Cu2 angle (89.7(2)°) which is more closed compared to 95.2(1)° in $[Cu_2(L_{OCH_3})(\mu\text{-OH})]^{2+}$ and 95.7(2)° in $[Cu_2(L_{CH_3})(\mu\text{-OH})]^{2+}$, the other angles in the Cu_2O_2 unit of $[Cu_2(L_F)(\mu\text{-OH})]$ are similar to those observed in the other μ-OH complexes. These results are however consistent with the intermetallic distance equal to 2.969(1) Å, which is in the same range as the Cu1···Cu2 distances measured for $[Cu_2(L_{OCH_3})(\mu\text{-OH})]^{2+}$ (2.980(9) Å) and $[Cu_2$-

(14) (a) Heany, H. In *Comprehensive Organic Synthesis*; Trost, B. M., Ed.; Pergamon: Oxford, U.K., 1991; Vol. 2, p 953. (b) Lubben, M.; Feringa, B. L. *J. Org. Chem.* **1994**, *59*, 2227−2233.

Table 2. Comparison of Main Interatomic Distances (Å) and Bond Angles (deg) in the Complexes $[Cu_2(L_{OCH_3})(\mu\text{-OH})]^{2+}$ and $[Cu_2(L_F)(\mu\text{-OH})]^{2+}$

	$[Cu_2(L_{OCH_3})(\mu\text{-OH})]^{2+}$	$[Cu_2(L_F)(\mu\text{-OH})]^{2+}$
Cu1−Cu2	2.980(9)	2.969(1)
Cu1−O2	1.913(3)	1.895(5)
Cu1−O1	1.997(3)	2.088(4)
Cu1−N3	2.245(4)	2.047(5)
Cu1−N1	2.023(4)	2.004(6)
Cu1−N4	2.010(4)	2.034(5)
Cu2−O2	1.905(3)	1.920(4)
Cu2−N2	2.030(4)	2.008(5)
Cu2−O1	2.039(3)	2.123(5)
Cu2−N5	2.018(4)	2.057(5)
Cu2−N6	2.120(4)	2.005(5)
Cu1−O1−Cu2	95.2(2)	89.7(2)
O1−Cu1−O2	81.5(1)	80.7(2)
O2−Cu1−N3	111.3(1)	100.4(2)
O2−Cu1−N1	167.6(1)	174.4(2)
O2−Cu1−N4	99.9(1)	99.7(2)
O1−Cu1−N3	99.7(1)	104.2(2)
O1−Cu1−N1	89.4(1)	94.2(2)
O1−Cu1−N4	154.4(1)	128.5(2)
N1−Cu1−N3	78.4(3)	83.0(2)
N3−Cu1−N4	103.4(1)	125.8(2)
N1−Cu1−N4	84.6(1)	81.8(2)
Cu1−O2−Cu2	102.6(1)	102.2(2)
O1−Cu2−O2	80.6(1)	79.2(2)
O2−Cu2−N2	172.9(1)	172.0(2)
O2−Cu2−N5	100.2(1)	100.6(2)
O2−Cu2−N6	102.9(2)	101.0(2)
O1−Cu2−N2	93.4(3)	93.2(2)
N2−Cu2−N1	81.8(1)	83.1(2)
N2−Cu2−N6	82.2(1)	82.0(2)
O1−Cu2−N5	138.8(3)	101.1(2)
O1−Cu2−N6	105.1(1)	129.4(2)
N5−Cu2−N6	114.6(1)	127.8(2)

$(L_{CH_3})(\mu\text{-OH})]^{2+}$ (2.966(1) Å). For both complexes, the spatial disposition of the pyridines relative to each other around the copper atoms makes the metal site easily accessible as observed for $[Cu_2(L_{CH_3})(\mu\text{-OH})]^{2+}$. The doubly bridged dicopper(II) complexes obtained from HL_F and HL_{OCH_3} ligands display nearly identical coordination structures close to the parent structure from HL_{CH_3} ligand. The R-substituent does not significantly affect the coordination sphere around the copper(II) (i.e., geometry, intermetallic distances, and bond lengths and angles). In a similar manner, on the phenoxo ring, the C−C bonds, and the C1−O1 bonds do not seem to be affected by the electronic effects of the various substituents.

(b) Complexes $[Cu_2(L_{CF_3})(H_2O)_2]^{3+}$ and $[Cu_2(L_F)(H_2O)_2]^{3+}$. The ORTEP views of the tricationic complexes are shown in Figure 3A ($[Cu_2(L_F)(H_2O)_2]^{3+}$) and Figure 3B ($[Cu_2(L_{CF_3})(H_2O)_2]^{3+}$). Selected bond lengths and angles are given in Table 3. It is worth noting that the complex $[Cu_2(L_{CF_3})(H_2O)_2]^{3+}$ is lying on a 2-fold axis (going through C5, C4, C1, and O1 atoms) as the complex $[Cu_2(L_{CH_3})(H_2O)_2]^{3+}$, while the complex $[Cu_2(L_F)(H_2O)_2]^{3+}$ is in general position but possesses a pseudo-2-fold axis involving the same structural characteristic than the two bis aqua complexes described here in. Each copper atom is pentacoordinated to the tertiary amine, two pyridine nitrogen atoms and the oxygen of the phenoxo bridge, and to an oxygen atom of water molecule. Contrary to the complexes $[Cu_2(L_R)(\mu\text{-OH})]^{2+}$, the two pyridine nitrogen atoms are trans to each other. The coordination polyhedron is a slightly distorded square pyramid whose apical position is occupied by the bridging phenoxo oxygen.

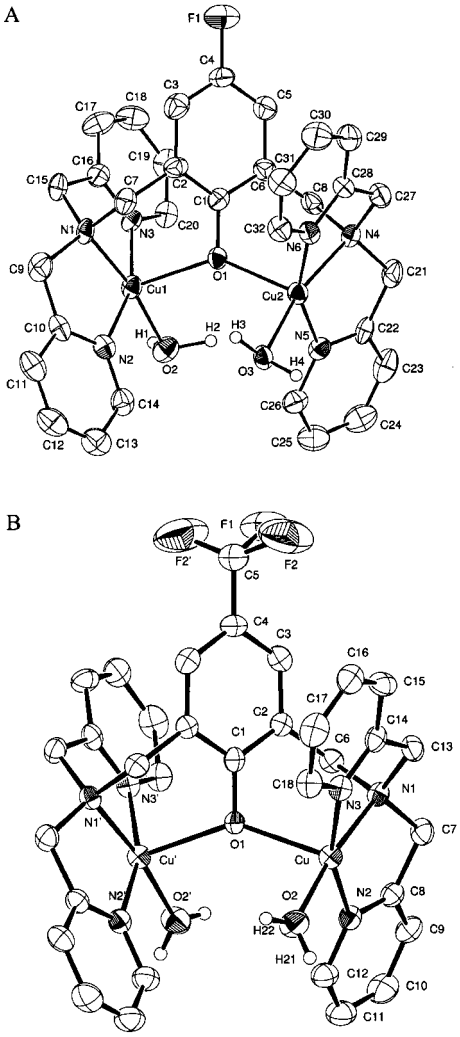

Figure 3. ORTEP plots of the tricationic units with atom labels and numbering scheme for (A) $[Cu_2(L_F)(H_2O)_2]^{3+}$ and (B) $[Cu_2(L_{CF_3})(H_2O)_2]^{3+}$. Hydrogens are omitted for clarity. Ellipsoids are drawn at the 30% probability level.

The square plane is defined by N1, N2, N3, and O2 atoms with a mean deviation to the least-squares plane of 0.060(5) Å for $[Cu_2(L_{CF_3})(H_2O)_2]^{3+}$ and 0.056(5) Å and 0.045(5) Å for the Cu1 and Cu2 surroundings in $[Cu_2(L_F)(H_2O)_2]^{3+}$, respectively. In $[Cu_2(L_{CF_3})(H_2O)_2]^{3+}$, the copper atoms lie 0.172(5) Å out of the basal plane toward the apical O1 atom, while the copper sites in $[Cu_2(L_F)(H_2O)_2]^{3+}$ are more distorted with distances from the mean planes of 0.2003(5) Å (Cu1) and 0.203(5) Å (Cu2). The axial distance Cu−O1 is longer (2.228(2) Å) in $[Cu_2(L_{CF_3})(H_2O)_2]^{3+}$ than those observed in $[Cu_2(L_F)(H_2O)_2]^{3+}$ (2.112(4) Å for Cu2 and 2.224(4) Å for Cu1). The copper−nitrogen distances are in the range of 1.992(5)−2.031(5) Å for $[Cu_2(L_{CF_3})(H_2O)_2]^{3+}$ and are quite close to those observed in $[Cu_2(L_F)(H_2O)_2]^{3+}$: 1.972(5)−2.009(5) Å for Cu1 and 1.976(5)−2.068(5) Å for Cu2, respectively. However it is interesting to note that the copper−aqua distances are really different since in $[Cu_2(L_{CF_3})(H_2O)_2]^{3+}$ the distance is 1.965(4) Å while in $[Cu_2$-

Table 3. Comparison of Main Interatomic Distances (Å) and Bond Angles (deg) in the Complexes $[Cu_2(L_F)(H_2O)_2]^{3+}$ and $[Cu_2(L_{CF_3})(H_2O)_2]^{3+}$

$[Cu_2(L_F)(H_2O)_2]^{3+}$		$[Cu_2(L_{CF_3})(H_2O)_2]^{3+}$	
Cu1−Cu2	4.084(1)	Cu−Cu′	4.222(2)
Cu1−O1	2.224(4)	Cu−O1	2.228(4)
Cu1−O2	2.002(4)	Cu−O2	1.965(4)
Cu1−N1	2.009(5)	Cu−N1	2.031(5)
Cu1−N2	1.976(5)	Cu−N2	1.992(5)
Cu1−N3	1.972(5)	Cu−N3	1.994(5)
Cu2−O1	2.112(4)		
Cu2−O3	2.010(4)		
Cu2−N4	2.068(5)		
Cu2−N5	1.976(5)		
Cu2−N6	1.998(5)		
Cu1−O1−Cu2	140.7(2)	Cu−O1−Cu′	142.6(3)
O1−Cu1−O2	95.6(2)	O1−Cu−O2	93.0(1)
O2−Cu1−N3	98.9(2)	O2−Cu−N3	99.0(2)
O2−Cu1−N1	170.6(2)	O2−Cu−N1	176.6(2)
O2−Cu1−N4	92.1(2)	O2−Cu−N4	93.4(2)
O1−Cu1−N3	93.1(2)	O1−Cu−N3	93.8(2)
O1−Cu1−N1	84.1(2)	O1−Cu−N1	83.4(2)
O1−Cu1−N4	161.2(2)	O1−Cu−N4	161.2(2)
N1−Cu1−N3	90.9(2)	N1−Cu−N3	93.0(2)
N3−Cu1−N4	83.8(2)	N3−Cu−N4	83.0(2)
N1−Cu1−N4	102.8(2)	N1−Cu−N4	100.4(2)
O1−Cu2−O3	97.2(1)		
O3−Cu2−N4	167.1(2)		
O3−Cu2−N5	92.5(2)		
O3−Cu2−N6	98.2(2)		
O1−Cu2−N4	95.5(2)		
N4−Cu2−N5	82.8(2)		
N4−Cu2−N6	82.4(2)		
O1−Cu2−N5	102.8(2)		
O1−Cu2−N6	95.3(2)		
N5−Cu2−N6	157.6(2)		

$(L_F)(H_2O)_2]^{3+}$ the distances are 2.002(4) Å for Cu1 and 2.010(4) Å for Cu2. This might be a consequence of the difference in the electron withdrawing power of F and CF_3 groups. In $[Cu_2(L_{CF_3})(H_2O)_2]^{3+}$ the bond angle Cu−O1−Cu′ is 142.6(3)° comparable to the 140.7(2)° of Cu1−O1−Cu2 in $[Cu_2(L_F)(H_2O)_2]^{3+}$. The phenolate ring in $[Cu_2(L_{CF_3})$-$(H_2O)_2]^{3+}$ is twisted relative to the Cu−O1−Cu′ plane with torsion angles Cu−O1−C1−C2 and Cu′−O1−C1−C2 equal to 53.5(3)°. In $[Cu_2(L_F)(H_2O)_2]^{3+}$ the twist is quite similar (54.7(6)°) for Cu1−O1−C1−C2 and (52.5(6)°) for Cu2−O1−C1−C6. The intermetallic distance observed in $[Cu_2$-$(L_{CF_3})(H_2O)_2]^{3+}$ (4.222(2) Å) is longer than the distances observed in $[Cu_2(L_{CH_3})(H_2O)_2]^{3+}$ (4.139(1) Å) and in $[Cu_2$-$(L_F)(H_2O)_2]^{3+}$ (4.084(1) Å).

Solution Studies. The copper(II) complexes obtained have been characterized in solution by UV−vis, ^{1}H NMR, and EPR spectroscopies.

(a) UV−Vis at 298 K (See Table 4). All complexes are characterized by a LMCT transition between the bridging phenolate and copper ions in the 340−470 nm region. For the μ-hydroxo and bis aqua complexes described here, the electron withdrawing fluorinated groups induce a neat hypsochromic shift, while the electron donating methoxyl group induces a bathochromic shift.[15] As previously shown[8] for the complexes from HL_{CH_3} the less strained open structure of the bis aqua complexes compared to the μ-hydroxo complexes induces a bathochromic shift of the LMCT transition, revealing a better overlap between the phenolate group orbital and the copper half-filled orbital, while for the λ_{max} of the d−d transitions a reverse shift is observed. These transitions are affected to a lesser extent by the electronic features of the substituent on the phenolic group. The position of these bands is more particularly affected by the geometry around the copper(II) and suggests a trigonal bipyramidal coordination for these μ-OH complexes. In the case of the bis aqua complexes, the d−d transition positions are in agreement with a square pyramidal geometry around the metal centers (see X-ray studies). Solution and solid-state structures remain very similar.

Table 4. UV−Vis and EPR Data for the Dicopper(II) Complexes

	UV−vis, λ_{max} (nm) (ϵ, M^{-1} cm^{-1})			
compound	d−d	LMCT	EPR[a] (g)	
$[Cu_2(L_{OCH_3})(\mu\text{-OH})]^{2+}$ [b]	787 (300)	440 (560)		
$[Cu_2(L_{CH_3})(\mu\text{-OH})]^{2+}$ [b,d]	785 (280)	410 (480)		
$[Cu_2(L_F)(\mu\text{-OH})]^{2+}$ [b]	781 (260)	410 (440)		
$[Cu_2(L_{CF_3})(\mu\text{-OH})]^{2+}$ [b]	806 (251)	340 (760)		
$[Cu_2(L_{OCH_3})(H_2O)_2]^{3+}$ [c]	691 (360)	460 (720)	4.35	2.12
$[Cu_2(L_{CH_3})(H_2O)_2]^{3+}$ [c,d]	700 (180)	460 (710)	4.36	2.13
$[Cu_2(L_F)(H_2O)_2]^{3+}$ [c]	693 (253)	441 (555)	4.33	2.12
$[Cu_2(L_{CF_3})(H_2O)_2]^{3+}$ [c]	701 (265)	380 (395)	4.36	2.13

[a] Spectral data given for $T = 77$ K and recorded in frozen solution of H_2O/DMSO (1/1 (v/v)). [b] CH_3CN solution (1.25×10^{-4} M at 25 °C), in H_2O solution, spectra are similar. [c] H_2O solution (1.25×10^{-4} M at 25 °C), in CH_3CN, changes in spectra indicate[8] the displacement of H_2O ligand by acetonitrile. [d] Reference 8.

(b) EPR Spectroscopy at 100 K. As previously observed with the complex of HL_{CH_3},[8] the three μ-hydroxo complexes are EPR-silent in solution and in the solid state, indicating a strong interaction between the two copper(II) atoms. This observation is consistent with a doubly bridged structure and the short copper−copper distance evidenced in the solid state for the $[Cu_2(L_R)(\mu\text{-OH})]^{2+}$ complexes. The intermetallic distances are in the same range (2.966(1), 2.969(1), and 2.980(9) Å respectively for R = CH_3, F, and OCH_3). The bis aqua dicopper complexes from HL_F, HL_{CF_3}, and HL_{OCH_3} in frozen solutions (H_2O/DMSO, 1/1) reveal two sets of signal at a $\Delta M_s = \pm 2$ transition from 100 to 200 mT and broad $\Delta M_s = \pm 1$ signal from 200 to 450 mT. Spectral parameters are given in Table 4 and spectra in Supporting Information (Figure S1). These values are consistent with the values observed for $[Cu_2(L_{CH_3})(H_2O)_2]^{3+}$ [8] with a distorded trigonal bipyramidal geometry around the Cu^{II} ions and suggest two coupled copper ions. The data differences observed (Table 4) indicate small geometrical changes between each bis aqua complex in accordance with the conclusion of the X-ray studies (see above).

(c) ^{1}H NMR Studies. The hydroxo-bridged complexes display similar spectra with relatively sharp and well-defined resonances (+180 to −40 ppm chemical shifts range in CD_3-CN). ^{1}H spectra and chemical shifts data are given in Supporting Information (Figure S2 and Table S1, respectively). The chemical shifts are easily attributed by reference to the spectrum of the complex derived from HL_{CH_3}.[8] The resonance of the μ-hydroxo protons which are exchanged with D_2O are observed when the spectra are recorded in

(15) Karlin, K. D.; Nasir, M. S.; Cohen, B. I.; Cruse, R. W.; Kaderli, S.; Zuberbühler A. D. *J. Am. Chem. Soc.* **1994**, *116*, 1324−1336.

Table 5. ^{19}F Chemical Shifts (ppm vs C_6F_6) in D_2O/DMSO (8/2, v/v)

	δF	
	R = F	R = CF_3
HL_R	32.0	100.8
$[Cu_2(L_R)(H_2O)_2]^{3+}$	65.5	110.4
$[Cu_2(L_R)(\mu\text{-OH})]^{2+}$	43.3	102.5
$[Cu_2(L_R)(OH)_2]^{+}$	51.5	a
$[Cu^{II}Cu^{I}(L_R)(OH)]^{+}$	22.7	nd[b]

[a] Instable in basic medium. [b] nd, not determined.

acetonitrile as solvent. Broad signals are observed in the paramagnetic region of the spectra for bis aqua complexes; the assignment of the remaining signals are given in Table S2 (Supporting Information). Thus, there is no particular correlation, as might be expected, between the observed chemical shifts and the R-substituent effect mediated in part through the phenoxo bridging ligand and somewhat influencing the magnetic properties of the complexes.[15]

(d) ^{19}F NMR Studies. The ^{19}F NMR may be an interesting tool to study the complexes derived from the fluorinated ligands. To our knowledge, there are only a few examples of ^{19}F NMR studies of paramagnetic copper complexes in the literature.[16] The ^{19}F chemical shifts measured for HL_F, HL_{CF_3} and for their complexes are given in Table 5. The mixed valence complex $[Cu^{II}Cu^{I}(L_F)(\mu\text{-OH})]^{+}$ has been obtained electrochemically (vide infra). It can also be obtained (in mixture) by reduction of the dicopper(II) complex with NaH (1 equiv) in acetonitrile. The complex $[Cu_2(L_F)(OH)_2]^{+}$ is given putatively; it has been obtained in basic medium (vide infra). The ^{19}F NMR spectra of the EPR silent μ-hydroxo complexes exhibit relatively sharp peaks, compared to the spectra of the bis aqua complexes which present broad resonance peaks. The CF_3 derivatives spectra exhibit peaks which are less broad than the peaks from the F derivatives, in accordance with the longer fluorine−metal distance and the well-known spin rotation contribution to relaxation of the faster rotating CF_3 group. Despite the fluorine atoms are far from the metal centers, ^{19}F chemical shifts are drastically dependent on the changes in the metal coordination spheres. Moreover, ^{19}F chemical shifts are an efficient probe of the redox states of the metal centers: a $\Delta\delta$ of 20.6 ppm is observed between the μ-hydroxo dicopper(II) complex from HL_F and the one-electron reduced corresponding complex.

(e) Electrochemical Results. The electrochemical behavior of complexes $[Cu_2(L_R)(\mu\text{-OH})]^{2+}$ and $[Cu_2(L_R)(H_2O)_2]^{3+}$ has been studied by cyclic voltammetry (CV) in CH_3CN + 0.1 M tetra-*n*-butylammonium perchlorate (TBAP). The electrochemical data are summarized in Table 6.

The CV curves recorded in CH_3CN solution of complexes formed between HL_R and Cu^{II} display in the negative region of potentials a reversible redox wave followed by an irreversible cathodic peak at a lower potential (Table 6; see Figure 4A for $[Cu_2(L_{CF_3})(\mu\text{-OH})]^{2+}$ as an example). Coulometric titrations by potentiostatic exhaustive electrolysis performed at a potential corresponding to the first electrochemical system give $n = 1$ exchanged electron per complex allowing to attribute this reversible signal to the $Cu_2^{II,II}/Cu_2^{II,I}$ redox couple. The mixed-valence $Cu_2^{II,I}$ species which is stable at the time scale of the CV (0.1 V s^{-1}) is reduced at a lower potential into the $Cu_2^{I,I}$ species which undergo a fast and irreversible decomposition. It must be noticed that studies of complexes containing aqua ligands in coordinating solvent like CH_3CN raises the question of solvent substitution. It can be assumed that, in CH_3CN medium, the initial labile H_2O ligands are partially replaced by solvent ones as previously shown with $[Cu_2(L_{CH_3})(H_2O)_2]^{3+}$.[8] This leads to the formation of complexes of the type $[Cu_2(L_R)(S)_2]^{3+}$ (S = H_2O and/or CH_3CN) at equilibrium. As a consequence, in the case of complexes formed between HL_R and Cu^{II}

Table 6. Electrochemical Data[a] in CH_3CN Medium

	oxidation data[c]		reduction data[c]
$[Cu_2(L_{CH_3})(\mu\text{-OH})]^{2+}$ [b]	0.75	−0.94	−1.24[d]
$[Cu_2(L_{CH_3})(H_2O)_2]^{3+}$ [b]	0.65	−0.33	−0.86[d]
$[Cu_2(L_F)(\mu\text{-OH})]^{2+}$	0.82[d]	−0.90	−1.30[d]
$[Cu_2(L_F)(H_2O)_2]^{3+}$	0.80[d]	−0.32	−1.14[d]
$[Cu_2(L_{CF_3})(\mu\text{-OH})]^{2+}$	1.10[d]	−0.86	−1.24[d]
$[Cu_2(L_{CF_3})(H_2O)_2]^{3+}$	1.12[d]	−0.78	−1.18[d]
$[Cu_2(L_{OCH_3})(OH)]^{2+}$	0.60	−0.95	−1.40[d]
$[Cu_2(L_{OCH_3})(H_2O)_2]^{3+}$	0.50	−0.35	−1.08[d]

[a] Measured by CV at 0.1 V s^{-1}. *E* vs $Ag/AgNO_3$ (10 mM) + CH_3CN + 0.1 M TBAP. [b] Reference 8. [c] $E_{1/2}$/V (reversible process) or E_p/V (irreversible process). [d] Irreversible.

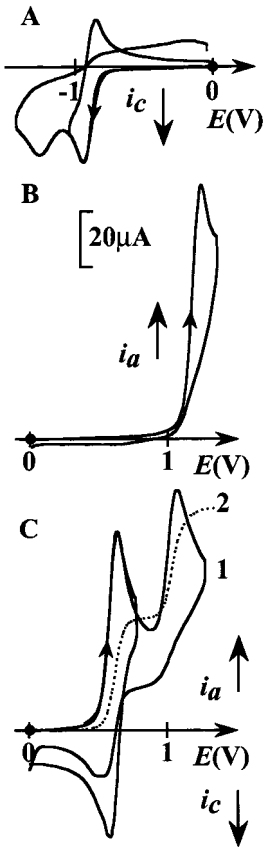

Figure 4. Voltammograms at a VC disk (5 mm diameter) of $[Cu_2(L_{CF_3})(\mu\text{-OH})]^{2+}$ (A, B), 2.2 mM, and $[Cu_2(L_{OCH_3})(\mu\text{-OH})]^{2+}$ (C (curve 1, CV curve; curve 2, electrochemical response at the VC RDE, 3 mm diameter, 600 rpm)), 3.0 mM, in CH_3CN + 0.1 M TBAP: scan rate, 0.1 V s^{-1}; *E* vs $Ag|Ag^{+}$; 10 mM CH_3CN + 0.1 M TBAP.

(16) Sobolev, A. V.; Krupoder, S. A.; Liskovskaya, T. I.; Danilovich, V. S. *J. Struct. Chem.* **2000**, *41*, 338−339.

containing aqua ligands, besides the main electrochemical signals, waves of weak intensity are detected on the CV curves.

Upon scanning toward the positive region of potentials, the CV curves recorded in electrolytic solutions of $[Cu_2(L_{OCH_3})(\mu\text{-OH})]^{2+}$ (Figure 4C, curve 1) and $[Cu_2(L_{OCH_3})(H_2O)_2]^{3+}$ exhibit a one-electron reversible wave at $E_{1/2} = 0.60$ and 0.50 V, respectively. It must be noticed that an additional electrochemical signal is seen at $E_{pa} = 1.16$ V as an irreversible peak in the case of $[Cu_2(L_{OCH_3})(\mu\text{-OH})]^{2+}$. The height of the corresponding waves recorded at the RDE (Figure 4C, curve 2) are similar allowing to attribute the second electrochemical signal to a one-electron transfer. The CV responses of complexes $[Cu_2(L_F)(\mu\text{-OH})]^{2+}$, $[Cu_2(L_F)(H_2O)_2]^{3+}$, $[Cu_2(L_{CF_3})(\mu\text{-OH})]^{2+}$ (Figure 4B), and $[Cu_2(L_{CF_3})(H_2O)_2]^{3+}$ are characterized by an irreversible oxidation wave at $E_{pa} = 0.82$, 0.80, 1.10, and 1.12 V, respectively. For all the complexes formed between HL_F or HL_{OCH_3} and Cu^{II} Coulometric titrations performed by exhaustive potentiostatic electrolysis, performed at a potential slightly greater than E_{pa}, show that all the anodic electrochemical responses are one-electron transfers (between 0.96 and 1.1 exchanged electron on repeated experiments). Thus, oxidation of $[Cu_2(L_R)X]^{n+}$ ($n = 2$, X = OH and $n = 3$, X = $(H_2O)_2$) leads in a first step to $[Cu_2(L_R)X]^{(n+1)+}$. The electron transfer is likely to be centered on the phenolate bridge as previously shown for other phenolate-bridged dicopper(II) complexes.[8] The oxidized $[Cu_2(L_{OCH_3})X]^{(n+1)+}$ complexes are stable at the time scale of the CV (0.1 V s^{-1}) as demonstrated by the reversibility of the corresponding electrochemical signals. Moreover, the solvent substitution in the complexes $[Cu_2(L_R)(H_2O)_2]^{3+}$ containing aqua ligands (see above) is not detected on the anodic part of the CV curves; i.e., substitution of H_2O by CH_3CN on the metal center does not influence significantly the electron transfer centered on the phenolate bridge. In addition, $[Cu_2(L_{OCH_3})(\mu\text{-OH})]^{2+}$ undergoes a supplementary irreversible electron transfer at $E_{pa} = 1.16$ V centered on the hydroxo bridge which is easier to be oxidized than the aqua ligands in $[Cu_2(L_{OCH_3})(H_2O)_2]^{3+}$.The same electrochemical behavior has been previously reported with $[Cu_2(L_{CH_3})X)^{n+}$ characterized by $E_{1/2} = 0.75$ V (X = OH, reversible) or 0.65 V ($X = (H_2O)_2$, reversible) and $E_{pa} = 1.26$ V (X = OH, irreversible).[8] The higher oxidation potential of $[Cu_2(L_F)(\mu\text{-OH})]^{2+}$ in association with the irreversibility of electron transfer preclude the observation of the second electron transfer. In the case of the complexes formed between L_{CF_3} and Cu^{II}, the Coulometric titration is elusive. As a matter of fact, the intensity of the anodic peaks at 1.10 and 1.12 V corresponding to the oxidation of $[Cu_2(L_{CF_3})(\mu\text{-OH})]^{2+}$ and $[Cu_2(L_{CF_3})(H_2O)_2]^{3+}$, respectively, does not correspond to a one-electron transfer. This can be due to the overlapping of the electrolytic solution oxidation and of the signal due to the complexes $HL_{CF_3} + Cu^{II}$ oxidation caused by its high oxidation potential. However, irreversible overoxidation of these complexes occurring at the same potential than the first electron transfer cannot be excluded.

The substitution on the phenol moiety of the ligands HL_R affects both the oxidation and reduction potentials of the corresponding complexes. However, it is more marked on the anodic features than on the cathodic ones, i.e., on the phenolate centered electron transfer than on the metal centered electron transfer. As example, the oxidation wave for the μ-hydroxo complexes is shifted from 0.60 V for the OMe derivatives (HL_{OCH_3}) up to 1.10 V for the CF_3 derivatives when it is located at 0.75 and 0.82 V for the Me and F derivatives, respectively. The first cathodic wave for the μ-hydroxo complexes with L_{OCH_3}, L_{CH_3}, L_F, and L_{CF_3} is found at -0.95, -0.93, -0.90, and -0.86 V, respectively. In addition the shift in potential according to the substitution is in agreement with the electron withdrawing or donating properties of the substituent on the phenol moiety. Compared to the CH_3 derivatives, the OCH_3 substituent is an electron donating group leading to a negative shift in the oxidation or reduction potential (e.g. -0.15 and -0.01 V respectively for the corresponding μ-hydroxo complexes) when the CF_3 (strong electron withdrawing group) substitution leads to a positive shift in potential for the electron transfer undergone by the corresponding complexes ($+0.35$ and $+0.08$ V, respectively). The same observation cannot be done for the second cathodic electron transfer undergone by all the studied complexes, probably due to the irreversibility of the corresponding electrochemical process. It must be noticed that substitution by the electron withdrawing group in HL_F and HL_{CF_3} causes a destabilization of the oxidized form of the complexes and therefore the irreversibility of the anodic electrochemical response. Another remark concerns the dependence of the exogen ligand on the electrochemical features of the complexes. Compared to the bis aqua complexes, the hydroxo bridge between the two copper metal centers induces a strong negative shift in the cathodic wave (ca -0.6 V for the complexes formed between HL_{CH_3,F,CF_3} and Cu^{II}) when a slight positive shift is observed for the oxidation wave (0.1 and 0.02 V for $Cu^{II} + HL_{OCH_3}$ and $Cu^{II} + HL_F$, respectively). This in agreement with the higher donor character of the μ-hydroxo ligand than the aqua one. In summary, the nature of the exogen ligand on the metal center (μ-hydroxo or aqua) affects more deeply the metal centered electron-transfer potential than the phenolate centered electron-transfer potential when it is the contrary for the substitution on the phenol moiety of the ligands.

(f) pH-Driven Interconversions in H_2O: p*K* Determinations. UV−vis titrations (data not shown), monitoring the LMCT band of the μ-hydroxo complexes with perchloric acid, lead quantitatively to the corresponding bis aqua complexes. Isosbestic points are observed, indicating, for each case, the presence of only two absorbing species, i.e. intermediates such as aquahydroxo dicopper(II) complexes, at equilibrium are not detectable. The reaction is fully reversible by addition of sodium hydroxide to the solutions of the bis aqua complexes (Figure 5, top). The method of Schwarzenbach[17] allows the determination of the apparent pK_1 (Table 7) for the species derived from HL_F, HL_{CF_3}, and HL_{OCH_3} (similar studies have been described for complexes from HL_{CH_3}[8]). Near pH = 10, the complex from HL_{CF_3} is

(17) Schwarzenbach, G.; Schwarzenbach, K. *Helv. Chim. Acta* **1963**, *46*, 1390−1400.

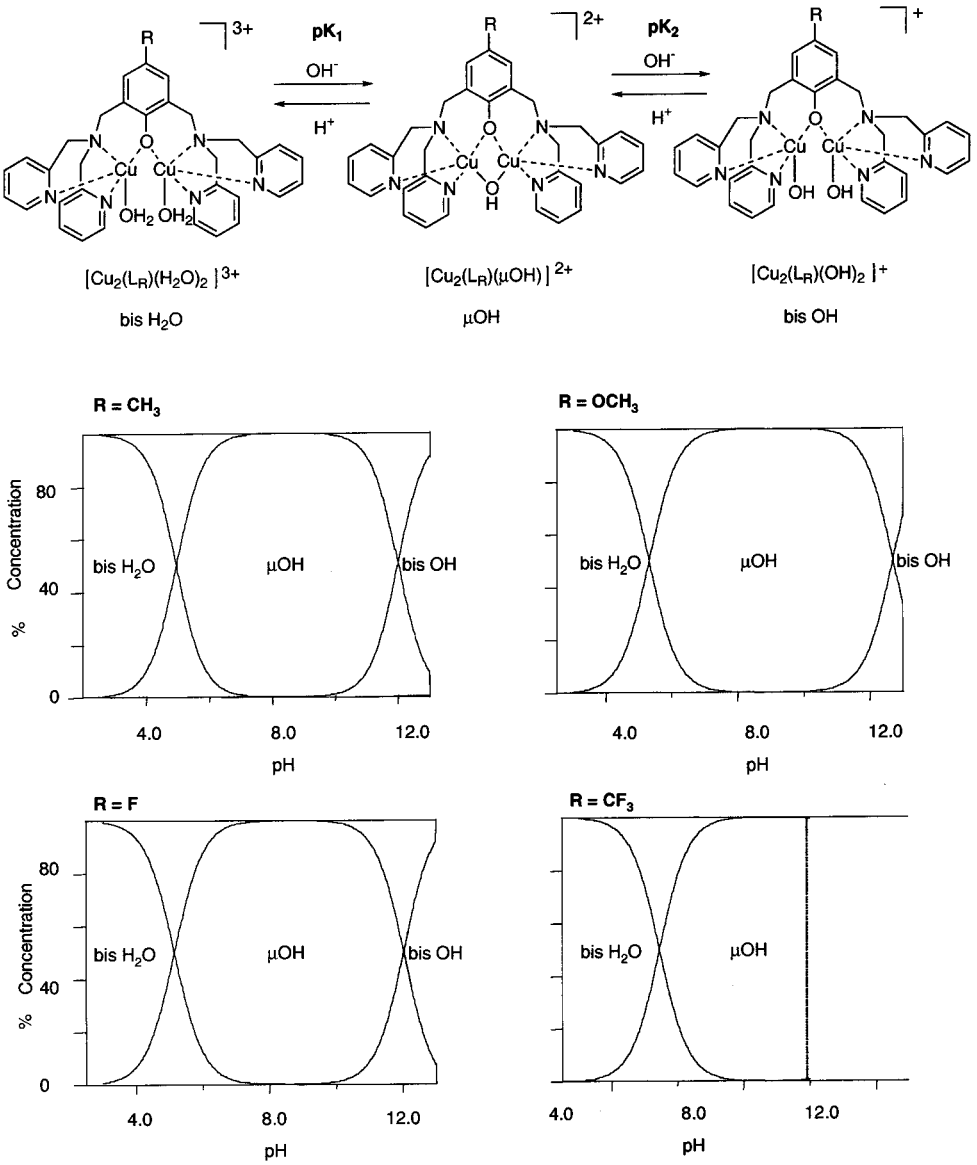

Figure 5. pH-driven interconversions between the complexes and species distribution curves as a function of pH for L_R complexes in aqueous solution.

Table 7. Deprotonation Constants (p*K*) for the Dinuclear Copper(II) Complexes in Aqueous Solution

R	pK_1	pK_2	pK_2 − pK_1
OCH_3	5.3	12.0	7.40
CH_3[a]	4.95	12.7	7.05
F	5.15	12.1	6.95
CF_3	5.45		

[a] Reference 8.

irreversibly transformed (see below). This could be correlated to the observed instability of 4-trifluorophenol moiety in basic medium. For the species derived from HL_F, and HL_{OCH_3}, as previously found with HL_{CH_3},[8] another species are reversibly formed in strong basic medium (pK_2 are reported in Table 7). These new compounds, which could not be obtained in the solid state, give UV−vis main features at 435 (ϵ = 1120), 420 (ϵ = 670), and 410 (ϵ = 920) nm for the species derived from HL_{OCH_3}, HL_{CH_3},[8] and HL_F, respectively, attributed to the LMCT phenoxo-to-copper(II) transition, and 700 (ϵ = 320), 700 (ϵ = 180), and 698 (ϵ = 330) nm attributed to Cu^{II} d−d transitions. These data suggest a square pyramidal coordination around the copper centers. The ^{1}H NMR (see, in Supporting Information, Table S2) and EPR spectra of these new species (Figure 6) are very similar to those observed for the bis aqua complexes. These similar features allow us to propose a (μ-phenoxo) (bis hydroxo) dicopper(II) structure for these species as previously done for the complex from HL_{CH_3} in basic medium.[8] Taking into account the difference between pK_2 and pK_1 (Table 7), it can be noticed that the pH range of stability of the μ-hydroxo complexes is in the order $L_{OCH_3} > L_{CH_3} > L_F > L_{CF_3}$. This influence of the para substituent on the bridging phenolate group follows the electronic properties: electron donating groups increase the stability of the μ-hydroxo complexes, while electron withdrawing groups decrease this stability.

The pH-driven interconversions were also studied by EPR spectroscopy at 100 K in frozen solutions of H_2O/DMSO (1/1 (v/v), 3mM). Results are depicted in Figure 6 in the case of the complexes from HL_{OCH_3}. Starting from the EPR-

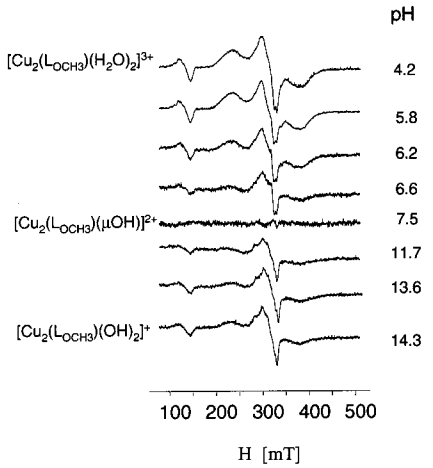

Figure 6. pH-driven changes of $[Cu_2(L_{OCH_3})(\mu\text{-OH})]^{2+}$ in EPR spectra at 100 K, in H_2O/DMSO (1/1 (v/v), 3mM). The microwave frequency is 9.4103 GHz. Both spectra were recorded with a microwave power of 20 mW, modulation frequency of 100 kHz, modulation amplitude of 0.2 mT, and one scan for 167 s. The pH was adjusted with $HClO_4$ or NaOH (1 M).

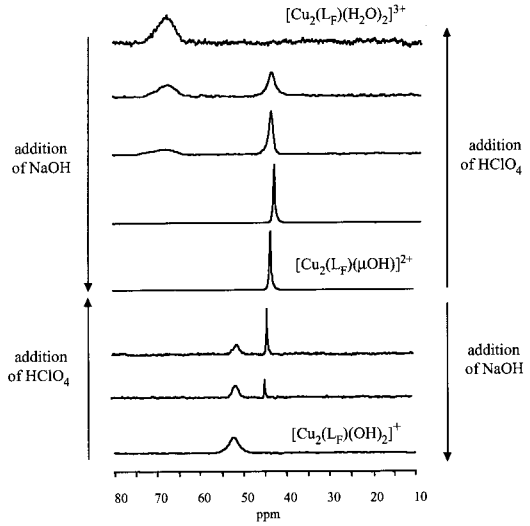

Figure 7. ^{19}F NMR monitored titration of $[Cu_2(L_F)(H_2O)_2]^{3+}$ by NaOH in D_2O/DMSO (8/2). (The same spectra are obtained by addition of $HClO_4$ to $[Cu_2(L_F)(\mu\text{-OH})]^{2+}$).

silent μ-hydroxo complex, a signal becomes detectable as the pH decreases, revealing a moderate coupling between the copper ions with a $\Delta M_s = \pm 2$ transition at 150 mT. Broad $\Delta M_s = \pm 1$ signals are observed near 200−440 mT. A similar trend for the pH range 7−14 is observed, revealing a moderate coupling between the two copper(II) ions.

These interconversions were further investigated by NMR spectroscopy. The μ-hydroxo complexes $[Cu_2(L_F)(\mu\text{-OH})]^{2+}$ in D_2O display ^1H NMR spectra with relatively sharp and well-defined resonances (0−180 ppm chemical shifts range). Decreasing (or increasing) the pH leads to a decrease in the intensity of the observed ^1H NMR signals, with a concomitant broadening in these signals. With the fluorinated complexes from HL_F and HL_{CF_3}, the pH-driven interconversions have been monitered by ^{19}F NMR. The spectra are depicted in Figures 7 and 8. Starting from the $[Cu_2(L_F)(\mu\text{-OH})]^{2+}$ spectrum, characterized by a single resonance at 43.3 ppm, addition of an increasing amount of $HClO_4$ in the

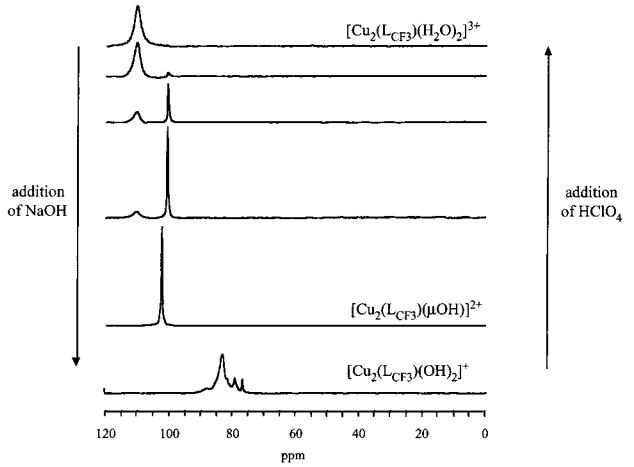

Figure 8. ^{19}F NMR monitored titration of $[Cu_2(L_{CF_3})(\mu\text{-OH})]^{2+}$ by $HClO_4$ in D_2O/DMSO (8/2).

solution leads to the appearance of a new signal which is clearly observed at 65.5 ppm. The new signal grows at the expense of the original resonance. In acid medium, only the new signal remains and it corresponds to the resonance found for the isolated $[Cu_2(L_F)(H_2O)_2]^{3+}$ (Table 5). The same behavior can be observed when an increasing amount of NaOH is added in the $[Cu_2(L_F)(\mu\text{-OH})]^{2+}$ solution (Figure 7). The direct mixing of HL_F, $Cu(ClO_4)_2$, and NaOH leads to the same complex (putatively $[Cu_2(L_F)(OH)_2]^{+}$) as that from the addition of NaOH to the characterized complex $[Cu_2(L_F)(\mu\text{-OH})]^{2+}$. The ($\mu$-phenoxo) (bis hydroxo) dicopper-(II) structure proposed for this species in basic medium are in accordance with results obtained by several methods (UV−vis, EPR, and ^1H and ^{19}F NMR titrations) that lead to similar conclusions. In particular, as previously established by UV−vis titration, no intermediate species, such as an aqua hydroxo dicopper(II) complex, are detected by ^{19}F NMR.

^{19}F NMR is proved to be a powerful tool for studying quantitatively the pH-dependent equilibrium between the various complexes. The equilibrium processes are slow at the ^{19}F NMR time scale, allowing the observation (and the quantitative measurements) of the species simultaneously present in the medium. It has to be emphasized that, in the same conditions, the exchange is fast with regard to the ^1H NMR time scale in relation with small chemical shift differences between the concerned chemical species.

Catechol Oxidase Activities. Catechol oxidases are type III copper proteins which catalyze the oxidation of catechols to quinones in the presence of oxygen.[18] As reported recently the crystal structure of the native *met*-form shows a mono-hydroxo bridged dicopper(II) active site.[19] Several $Cu^{II}Cu^{II}$-based models with catechol oxidase activity have been described.[20−32] In the first systematic study, Nishida et al.[20]

(18) Eicken, C.; Krebs, B.; Sacchettini, J. C. *Curr. Opin. Struct. Biol.* **1999**, *9*, 677−683.
(19) Klabunde, T.; Eicken, C.; Sacchettini, J. C.; Krebs, B. *Nat. Struct. Biol.* **1998**, *5*, 1084−1090.
(20) Oishi, N.; Nishida, Y.; Ida, K.; Kida, S. *Bull. Chem. Soc. Jpn.* **1980**, *53*, 2847−2850.
(21) Gentschev, P.; Möller, N.; Krebs, B. *Inorg. Chim. Acta* **2000**, *300*, 442−452.
(22) Reim, J.; Krebs, B. *J. Chem. Soc., Dalton Trans.* **1997**, 3793−3804.

Table 8. Catalytic Activities for $[Cu_2(L_R)(\mu\text{-OH})]^{2+}$ Complexes

R	V_{max} (10^{-6} $M^{-1}\cdot s^{-1}$)	K_M (mM)	turnover no. (90 mn)
OCH_3	2.2	0.25	32
CH_3[a]	1.1	1.49	16
F	0.27	8.8	8
CF_3	0	0	0

[a] Reference 8.

pointed out that dinuclear copper(II) complexes show a high catalytic activity compared to mononuclear complexes and proposed that a determining factor is the presence of two metal centers located in close proximity to facilitate the binding of the two oxygen atoms of the catechol prior to the electron transfer. Our previous studies[8] on the catalytic oxidation of catechol performed with dicopper(II) complexes from HL_{CH_3} showed that the catecholase activities are drastically dependent on the copper−copper distance which was modified upon pH-induced changes in the coordination sphere of the complex. It seemed interesting to compare the activity of the complexes described in this paper, with the aim of correlating the results with the structural and electronic parameters induced by the substituent in the para position of the bridging phenolate group. 3,5-Di-*tert*-butylcatechol (3,5-DTBC), the most widely used substrate, has been employed; the activities and reaction rates have been determined in acetonitrile by following the appearance of the absorption maximum of the quinone (3,5-DTBQ) at 410 nm overtime, under an atmosphere saturated with O_2. The reaction rate was obtained from the slope of the trace at 410 nm and Lineweaver−Burk treatment. Results of the oxidation studies are presented in Table 8. Large differences in the catalytic activities of the complexes are observed. *Only the μ-hydroxo complexes from HL_{CH3}, HL_F, and HL_{OCH3} exhibit a catecholase activity*. All the complexes from HL_{CF_3} are inactive. For the more active species, the catalytic activity are in the range of those observed for dicopper(II) complexes described in the literature.[20−32] Addition of a small amount of acid or base stopped the catecholase activity which was fully restored when the pH was adjusted to 6−8, i.e. in the range where the μ-hydroxo complexes are the only species present in solution. As observed in the X-ray structures of the μ-hydroxo complexes (R = OCH_3, CH_3, or F) the metallic centers are easily accessible (less steric bulk around the copper atoms in trigonal geometry) and the short Cu−Cu distance (≈2.9 Å in μ-hydroxo complexes versus ≈4 Å in the bis aqua complexes) allows a bridging catechol coordination compatible with the distance between the two *o*-diphenol oxygen atoms. Similar conclusions have been previously done by Krebs.[22] It is worth noting that the intermetallic distance is 2.9 Å in the oxidized enzyme, which is characterized by a μ-hydroxo dicopper(II) active site.[19]

On the other hand the catecholase activity of the μ-hydroxo complexes is drastically modulated by the substituent in the para position of the bridging phenolate moiety: taking the methyl-substituted ligand as a reference, substitution by the poorly electron withdrawing fluorine atom inhibits to a moderate extent the activity while substitution by the donating methoxyl group increases notably the activity in the μ-OH dicopper(II) complexes. These results evidence that the catalytic properties of the complexes depend on the electronic effects reflected by the redox potential values determined for the μ-OH dicopper(II) complexes (Table 6), even if it's clear that electronic effects do not control solely the reactivity. In particular, as previously shown for the complexes from HL_{CH_3}, the redox potential of the dicopper complexes are not decisively related to the observed activities, since bis aqua complexes are more easily reduced than the μ-hydroxo complexes.

It should be stressed that substitution by the strongly electron withdrawing trifluoromethyl group completely inhibits the activity of the corresponding μ-OH complex, although $[Cu_2(L_{CF_3})(\mu\text{-OH})]^{2+}$ possesses similar structural features than the other μ-OH active complexes. Catechol binding studies investigated by UV−vis spectroscopy with tetrachlorocatechol (TCC, a non-easily oxidable catechol) or with 3,5-DTBC in anaerobic conditions, show that the $[Cu_2(L_{CF_3})(\mu\text{-OH})]^{2+}$ complex does not bind catechols. This demonstrates that the formation of an intermediate between the catechol and the Cu^{II} complex prior to electron transfer is a key step. Applying the Michaelis−Menten approach, the K_M parameters have been determinated. The values (Table 8) are associated with the ability of the complex to form an adduct with the substrate and are not correlated directly with the electronic effects from R-groups (it can be noticed that the v_{max} values are correlated with the Hammett σ_p values). Several parameters are involved in the catalytic efficiency of these complexes, especially intermetallic distance, geometry, and steric features around the copper atoms and redox potential, modulated herein by the pH and the electronic features of the R-substituent on the ligand to lead to an optimal interaction between the copper(II) complexes and the substrate.

Conclusion

Substitution of the methyl group of the H-BPMP ligand by electron withdrawing (F or CF_3) or electron donating (OCH_3) groups induces changes in the properties of the corresponding dicopper complexes. Structural, spectroscopic, redox properties and pH-driven interconversions have been studied, as well as the catecholase activities. The R-substituent on the ligand induces a drastic effect on the

(23) Monzani, E.; Battaini, G.; Perotti, A.; Casella, L.; Gullotti, M.; Santagostini, L.; Nardin, G.; Randaccio, L.; Geremia, S.; Zanello, P.; Opromolla, G. *Inorg. Chem.* **1999**, *38*, 5359−5369.
(24) Monzani, E.; Quinti, L.; Perotti, A.; Casella, L.; Gullotti, M.; Randaccio, L.; Geremia, S.; Nardin, G.; Faleschini, P.; Tabbi, G. *Inorg. Chem.* **1998**, *37*, 553−562.
(25) Parimala, S.; Gita, K. N.; Kandaswamy, M. *Polyhedron* **1998**, *17*, 3445−3453.
(26) Malachowski, M. R.; Dorsey, B. T.; Parker, M. J.; Adams, M. E.; Kelly, R. S. *Polyhedron* **1998**, *17*, 1289−1294.
(27) Malachowski, M. R.; Huynh, H. B.; Tomlinson, L. J.; Kelly, R. S.; Furbee, J. W., Jr. *J. Chem. Soc., Dalton Trans.* **1995**, 31−36.
(28) Malachowski, M. R.; Tomlinson, L. J.; Davidson, M. G.; Hall, M. J. *J. Coord. Chem.* **1992**, *25*, 171−174.
(29) Zippel, F.; Ahlers, F.; Werner, R.; Haase, W.; Nolting, H. F.; Krebs, B. *Inorg. Chem.* **1996**, *35*, 3409−3419.
(30) Than, R.; Feldmann, A. A.; Krebs, B. *Coord. Chem. Rev.* **1999**, *182*, 211−241.
(31) Börzel, H.; Comba, P.; Pritzkow, H. *Chem. Commun*. **2001**, 97−98.
(32) Gupta, M.; Mathur, P.; Butcher, R. J. *Inorg. Chem.* **2001**, *40*, 878−885.

catecholase activity of the corresponding μ-OH dicopper(II) complexes. The substitution by an electron donating group increases this activity, while the substitution by an electron withdrawing group has the reverse effect. $[Cu_2(L_{OCH_3})(\mu\text{-OH})]^{2+}$ proved to be the most active complex among the studied models, showing that a simple synthetic modification of the ligand may be used to modulate the catalytic abilities of the complexes. Further studies are in progress concerning the detailed mechanism of the catechol oxidase activity of the μ-hydroxo complexes.

With the fluorinated ligands, the ^{19}F NMR proved to be a powerful tool for the studies of the complexes. The fluorine chemical shifts are a good probe of the changes in the coordination sphere of the copper centers and of their redox states. Moreover, ^{19}F NMR time scale allowed the observation of different species in equilibrium, in conditions where the exchange is fast with regard to the ^1H NMR time scale. The use of fluorine-labeled ligands seems to be a very promising approach for the study of metal complexes.

Acknowledgment. The authors are grateful to Dr. Alain Deronzier for his interest in this work, to Dr. André Jeunet for his assistance in the EPR spectroscopic studies, and to Guy Serratrice for fruitful discussions.

Supporting Information Available: ^1H NMR resonance assignments for $[Cu_2(L_R)(\mu\text{-OH})]^{2+}$ (Table S1) and for $[Cu_2(L_R)(H_2O)_2]^{3+}$ and $[Cu_2(L_R)(OH)_2]^{+}$ complexes (Table S2), EPR spectra for $[Cu_2(L_R)(H_2O)_2]^{3+}$ complexes (Figure S1), and ^1H NMR of $[Cu_2(L_R)(\mu\text{-OH})]^{2+}$ complexes (Figure S2). Complete tables of atomic parameters and bond lengths and angles are available in CIF format. This material is available free of charge via the Internet at http://pubs.acs.org.

IC010534G